MOLECULAR AND CELLULAR BIOLOGY, May 2000, p. 3245–3255 Vol. 20, No. 9
0270-7306/00/$04.00+0

A Novel Family of Cell Wall-Related Proteins Regulated Differently during the Yeast Life Cycle

JOSÉ MANUEL RODRÍGUEZ-PEÑA, VÍCTOR J. CID, JAVIER ARROYO,* AND CÉSAR NOMBELA

Departamento de Microbiología II, Facultad de Farmacia, Universidad Complutense de Madrid, 28040 Madrid, Spain

Received 21 June 1999/Returned for modification 19 August 1999/Accepted 4 February 2000

The *Saccharomyces cerevisiae* Ygr189c, Yel040w, and Ylr213c gene products show significant homologies among themselves and with various bacterial β-glucanases and eukaryotic endotransglycosidases. Deletion of the corresponding genes, either individually or in combination, did not produce a lethal phenotype. However, the removal of *YGR189c* and *YEL040w*, but not *YLR213c*, caused additive sensitivity to compounds that interfere with cell wall construction, such as Congo red and Calcofluor White, and overexpression of *YEL040w* led to resistance to these compounds. These genes were renamed *CRH1* and *CRH2*, respectively, for Congo red hypersensitive. By site-directed mutagenesis we found that the putative glycosidase domain of *CRH1* was critical for its function in complementing hypersensitivity to the inhibitors. The involvement of *CRH1* and *CRH2* in the development of cell wall architecture was clearly shown, since the alkali-soluble glucan fraction in the *crh1*Δ *crh2*Δ strain was almost twice the level in the wild-type. Interestingly, the three genes were subject to different patterns of transcriptional regulation. *CRH1* and *YLR213c* (renamed *CRR1*, for *CRH* related) were found to be cell cycle regulated and also expressed under sporulation conditions, whereas *CRH2* expression did not vary during the mitotic cycle. Crh1 and Crh2 are localized at the cell surface, particularly in chitin-rich areas. Consistent with the observed expression patterns, Crh1–green fluorescent protein was found at the incipient bud site, around the septum area in later stages of budding, and in ascospore envelopes. Crh2 was found to localize mainly at the bud neck throughout the whole budding cycle, in mating projections and zygotes, but not in ascospores. These data suggest that the members of this family of putative glycosidases might exert a common role in cell wall organization at different stages of the yeast life cycle.

The cell wall preserves the osmotic integrity of fungal cells and determines cellular morphology during various developmental processes. In the budding yeast *Saccharomyces cerevisiae*, the cell wall must exert its protective role during budding, mating, sporulation, and pseudohyphal growth, showing different morphogenetic patterns that obey diverse environmental conditions. The rapid growth of buds or mating projections, for instance, suggests that the accurate dynamics that rule the development of such an apparently rigid structure may allow a certain flexibility, at least in growing areas, without altering the protective function of the cell wall.

The budding yeast cell wall is basically constituted by highly mannosylated proteins (mannan) and three kinds of polysaccharide chains: (i) the predominant, linear 1,3-β-glucan, (ii) a minor, highly branched 1,6-β-glucan component, and (iii) chitin. Glucans make up about half of the dry weight of the cell wall, while chitin accounts for only 1 to 2%. Although cells can survive when deprived of the bulk of chitin (45), this *N*-acetylglucosamine polymer is essential for the formation of a proper primary septum during cytokinesis and for the characteristic ring-like structures at the mother-bud neck that leave a scar on the mother cell wall after cell division (45). Chemical treatment of isolated yeast cell walls yields an alkali-soluble fraction, rich in 1,3-β-glucan, and a major acid- and alkali-insoluble β-glucan fraction that also retains most of the 1,3-β-glucan (8). This insolubility has been explained in terms of its covalent linkage to chitin (15), and the nature of this linkage has been found to be a 1,4-β-glycosidic bond (26).

Careful biochemical approaches have provided evidence that the different components of the yeast cell wall are covalently linked in vivo as macromolecular complexes, constituting what has been called the "flexible building block," in which mannoproteins would be linked by the remnant of their glycosylphosphatidylinositol (GPI) anchor moieties to 1,6-β-glucan, which in turn is bound to 1,3-β-glucan core chains (23, 27). According to the model proposed by these authors, chitin could bind either 1,3- or 1,6-β-glucan, thus completing the hypothetical block. Several of the connections between these components through various types of glycosidic linkages are now known in detail (26, 27). A stoichiometric relationship of the cell wall components in such a basic unit is hard to assess and probably varies in different areas of the wall and under different morphogenetic programs.

A vast array of valuable information has been gathered on the genetic and biochemical characterization of the enzymes responsible for cell wall biosynthesis, including glucan and chitin synthases, chitinases, and exo- and endo-β-glucanases (for recent reviews, see references 29 and 36). However, the involvement of these enzymes in the construction and maintenance of the cell wall in vivo remains mostly obscure. In particular, little is known about which enzymes are responsible for cross-linking between cell wall polymers. Cross-linking among mannoproteins, β-glucans, and chitin may indeed account for the plastic properties of the cell wall during different developmental processes. A critical step for obtaining further insight into the mechanisms involved in cell wall assembly will be to identify these cross-linking enzymes, determine how these proteins work, and find out how the cell wall architecture is modified during the yeast cell cycle.

With the yeast genome sequenced, candidates can be sought from among predicted proteins that bear sugar-binding consensus sites or display a certain degree of homology with known transglycosidases from other organisms. Here we report

* Corresponding author. Mailing address: Departamento de Microbiología II, Facultad de Farmacia, Universidad Complutense de Madrid, 28040 Madrid, Spain. Phone: 34 91 3941746. Fax: 34 91 3941745. E-mail: jarroyo@eucmax.sim.ucm.es.

TABLE 1. Oligonucleotides used in this study

Oligonucleotide	Sequence
For ORF *YEL040W*[a]	
S1	5′ ATTTATTGTCCTGCAAATAAGCTAATTATATAATTAATAATGCGTACGCTGCAGGTCGAC 3′
S2	5′ GTCCTGTGTAGCCTATTTGTTCTTAGATGCAGATCCTCCTAATCGATGAATTCGAGCTCG 3′
V1	5′ CCGTGCGGCCATCAAAATG 3′
V2	5′ CGGACTCGTCAGGCTCATTT 3′
V3	5′ CGTCGGAGGAGATATTTATTA 3′
V4	5′ GCCCAGATGCGAAGTTAAG 3′
For ORF *YLR213c*[b]	
S1	5′ TTAGAGTATCATCAAGGGCTTTTGCACGAAATAAAAATATGTGTGGGAATACTCAGGTAT 3′
S2	5′ TACGGAAGAGAGAACTTCGTAAGACATTATTGCTGTGACTACCTATGAACATATTCCATT 3′
V1	5′ CGGCCTCTCACCTTTCCTTT 3′
V2	5′ CGGCGTGAATATGCGAGAAAT 3′
V3	5′ CTGGAATCAGGAAGCTGAGAT 3′
V4	5′ GCTGTCGCCGAAGAAGTTAA 3′
For site-directed mutagenesis of *YGR189c*[c]	
A1	5′ CCACCGTCAGCTTCAATAGAT 3′
A2	5′ TTGGATGAAATT**A**ATATT**C**AATGGGTGG 3′
A3	5′ CCACCCATT**G**AATAT**T**AATTTCATCCAA 3′
A4	5′ CAGCTTCTAGCACTGCTTCGT 3′
For *Spe*I-GFP cassette[d]	
N-GFP	5′ GCACTAGTCCA**AGTAAAGGAGAAGAACTT** 3′
C-GFP	5′ GGACTAGTTGG**TTTGTATAGTTCATCCAT** 3′

[a] The sequence complementary to the *HIS3* cassette is underlined.
[b] The sequence complementary to the *LEU2* cassette is underlined.
[c] Nucleotides changed with respect to the original sequence are underlined and boldfaced.
[d] *Spe*I restriction sites are underlined. The nucleotides belonging to the GFP ORF are boldfaced, including, respectively, the second codon and the one before the STOP codon.

the existence of a novel family of three putative yeast glycosidases. Characterization of strains with knockouts of these genes suggests their participation in cell wall assembly. Cell cycle expression studies and localization of the gene products at different development stages suggest a specific temporal and spatial role for each gene in cell wall construction.

MATERIALS AND METHODS

Strains and growth media. All experiments were performed with the *S. cerevisiae* FY1679 strain (*MAT***a**/α *ura3-52/ura3-52 his3Δ200/HIS3 leu2Δ1/LEU2 trp1Δ63/TRP1 GAL2/GAL2*) and haploid derivatives. To assess the mating type of the segregants, they were mated to strains 1783 (*MAT***a** *ura3Δ52 leu2-3,112 trp1-1 his4 can1*) and 1784 (*MAT*α *ura3Δ52 leu2-3,112 trp1-1 his4 can1*). The FY1679 *ygr189c*::*KanMX4* disruptant strain was obtained previously (40). Strains 19Δ2-37d (*MAT***a** *chs1 leu2 trp1 ura3 chs2*::*LEU2*) and HVY244 (*MAT*α *ura3 his1 leu2 chs3*::*LEU2*) were kindly provided by A. Durán. For routine cultures, *S. cerevisiae* was grown on YED (2% yeast extract and 2% glucose) or YEPD (YED plus 2% peptone). When required, glucose was replaced by other carbon sources in the same proportion. To induce sporulation, diploid cells were grown for 24 h in solid presporulation medium (5% glucose, 1% yeast extract, 3% meat extract) and then for 5 days in solid sporulation medium (1% potassium acetate plus sufficient amounts of histidine, tryptophan, leucine, adenine, and uracil). To synchronize cultures with mating pheromone, α-factor (Sigma) was added to exponentially growing cells to a final concentration of 10 μg/ml and incubated for 3 h. After this time, cells were collected, washed, resuspended in fresh YEPD, and incubated so as to resume growth. Both shmoo formation and culture synchronicity in the first cycle after release from pheromone-induced arrest were followed by phase-contrast microscopy. The *Escherichia coli* strain used as the plasmid host was DH5α (*supE44 ΔlacU169* (ϕ80 *lacZ*ΔM15) *hsdR17 recA1 endA1 gyrA96 thi-1 relA1*). For selective growth, bacteria were grown on Luria-Bertani (LB) medium containing 100 mg of ampicillin/liter.

Yeast genetics and phenotypic analyses. Tetrad analyses were performed by standard micromanipulation procedures. Markers of the segregants were verified on SD (20 g of glucose/liter, 1.67 g of yeast nitrogen base without amino acids/liter, 5 g of ammonium sulfate/liter, and the appropriate amount of amino acids) plates lacking a particular amino acid. The sensitivity or resistance of the segregants to Geneticin (encoded by the *KanMX4* module) was studied on YEPD plates containing 200 mg of Geneticin/liter. Calcofluor white (fluorescent brightener 28; Sigma) and Congo red (Merck) sensitivities were tested by spotting cells onto plates. Cells were grown overnight in YED or SD-Ura and adjusted to an optical density at 600 nm (OD_{600}) of 0.13 (approximately 2×10^3 cells per μl). Five microliters of samples plus two serial 1/10 dilutions were deposited on the surfaces of solid media supplemented with various concentrations of Calcofluor white or Congo red. Growth was monitored after 2 to 3 days at 28°C.

Cell polarity and morphogenetic defects were evaluated by fluorescence microscopy after cell wall chitin was stained with Calcofluor white as described elsewhere (38).

Molecular biology techniques. Standard molecular biology techniques for DNA manipulations and bacterial transformations were used as described elsewhere (43). Restriction enzymes were provided by Boehringer-Mannheim. In the construction of *YEL040w* and *YLR213c* deletant strains, the complete open reading frame (ORF) was deleted, except for the start and stop codons. Disruptions were performed by the SFH (short flanking homology) PCR technique (50), which allows the replacement of the target ORF by a selection marker. For *YEL040W* deletion, the *HIS3* marker from plasmid pFA6a-His3MX6 (see Table 2) was used, and for *YLR213c* deletion, we used the *LEU2* marker from the YEplac181 plasmid (see Table 2). The oligonucleotides devised for this purpose are listed in Table 1. S1 primers bear 41 to 42 nucleotides homologous to the upstream sequence of the target ORF plus 18 to 19 nucleotides of the marker module. S2 primers bear 41 nucleotides downstream from the target ORF plus 19 nucleotides of the marker module. The SFH deletion cassettes were obtained by using the Expand High Fidelity PCR System (Boehringer Mannheim). ORF replacements were identified by PCR with the help of diagnostic primers which bind either outside the target ORF (V2 and V3) or within the selection marker (V1 and V4). PCRs were carried out with the primer pairs V1–V2 and V3–V4 using Biotaq DNA Polymerase (BIOLINE).

The plasmids developed in this work are listed in Table 2. When necessary, sequence verification of the clones was carried out on an automated DNA sequencer (ALF [Pharmacia] and ABI 377 [Applied Biosystems]). Yeast transformation was carried out by the lithium acetate protocol (12). Ura^+ transformants were selected on SD-Ura plates. Doxycycline (10 mg/liter; Sigma) was added when required.

RNA analysis. Total RNA was isolated from exponentially growing cells in YEPD medium by the acidic phenol method as described previously (2). Samples were also taken from YEPG medium (YEPD in which glucose had been replaced by galactose) under the same conditions and from sporulation medium after 24 h of incubation. Samples were run in a morpholinepropanesulfonic acid (MOPS)-formaldehyde agarose gel and transferred by capillarity to a Nytran nylon mem-

TABLE 2. Plasmids used in this work

Plasmid	Relevant characteristics	Source or reference
pRS416	Centromeric vector; *URA3*; Amp^r	46
pEGH059	Cosmid containing a 39-kb DNA fragment from chromosome VII of *S. cerevisiae* S288C inserted into the vector pWE15	1
YEp352	Episomic vector; *URA3*; Amp^r	17
pBluescript KS	pUC19-derived phagemid; Amp^r	Stratagene
pT7Blue	Cloning vector; Amp^r	Novagen
pCM190	Doxycycline-regulatable expression; episomic vector; *URA3*; Amp^r	10
YEplac181	Episomic vector; *LEU2*; Amp^r	11
pFA6b-GFP(S65T)-KanMX6	Plasmid bearing the GFP-S65T coding sequence lacking the ATG, fused to the *S. cerevisiae ADH1* terminator	50
pFA6a-His3MX6	Plasmid containing a module for PCR gene disruption, including a heterologous *HIS3* marker	50
pAB25	Plasmid containing *YEL040w*	F. Sherman (32)
pJV89C	2.1-kb *Cla*I/*Dra*I fragment from the pEGH059 cosmid subclone E3[a] inserted into *Cla*I/*Dra*I-cleaved pRS416	This work
pJV89E	*Bam*HI/*Xho*I from pJV89C inserted into *Bam*HI/*Sal*I-cleaved Yep352	This work
pJV89G	733-bp *Spe*I-GFP-*Spe*I cassette generated by PCR[b] from plasmid pFA6b-GFP(S65T)-KanMX6 inserted in-frame into *Spe*I-cleaved pJV89E	This work
pJV89M	481-bp *Mam*I/*Spe*I fragment from site-directed mutagenesis by PCR of pJV89E[b] subcloned into *Mam*I/*Spe*I-cleaved pJV89E	This work
pJV40C	2.4-kb *Sca*I/*Xho*I fragment from pAB25 inserted into *Sma*I/*Xho*I-cleaved pRS416	This work
pJV40E	*Bam*HI/*Xho*I from pJV40C inserted into *Bam*HI/*Sal*I-cleaved YEp352	This work
pJV40G	733-bp *Spe*I-GFP-*Spe*I cassette generated by PCR[b] from plasmid pFA6b-GFP(S65T)-KanMX6 inserted in-frame into *Spe*I-cleaved pJV40E	This work
pJV40A	388-bp *Asn*I/*Kpn*I fragment from pJV40E inserted into *Nde*I/*Kpn*I-cleaved pT7-Blue	This work
pJV40B	1.3-kb *Kpn*I fragment from pJV40E inserted into *Kpn*I-cleaved pJV40A	This work
pJV40D	*Sac*I/*Xba*I from pJV40B inserted into *Sac*I/*Xba*I-cleaved pBluescript KS	This work
pJV40S	1.5-kb *Bam*HI/*Nsi*I fragment (promoterless *YEL040w*) from pJV40D inserted into *Bam*HI/*Pst*I-cleaved pCM190	This work

[a] See reference 1.
[b] See the text.

brane (Schleicher & Schuell) as described previously (43). The transferred RNA was cross-linked to the membrane by a 5-min exposure to UV light at 254 nm and hybridized with [α-^{32}P]dCTP (Amersham)-labeled probes. A 1.2-kb *Spe*I/*Eco*RV DNA fragment containing the *YGR189c* coding region, a 1.3-kb *Dra*I/*Spe*I DNA fragment containing the *YEL040W* coding region, and a 1.4-kb *Bam*HI/*Cla*I DNA fragment containing the *YLR213c* coding region were used as probes to detect their corresponding transcripts. As a reference for normalization of the procedure, a 1.6-kb *Bam*HI/*Hin*dIII DNA *ACT1*-containing fragment was used as a control probe. A Fluor-S MultiImager (Bio-Rad) was used to quantify the radioactive signal on autoradiograms.

Construction of GFP fusions. In order to create fusion proteins of both Ygr189c and Yel040w with the green fluorescent protein from *Aequorea victoria* (GFP), we took advantage of a unique *Spe*I site that exists in frame in both genes. The GFP cassette (733 bp) was synthesized by PCR using oligonucleotides N-GFP and C-GFP (see Table 1). The cassette was flanked by two *Spe*I restriction sites, which were used to insert it in frame into both genes. A triplet coding for proline before and after the GFP-coding sequence was included. The pFA6b-GFP(S65T)-KanMX6 plasmid (Table 2) was used as a template in PCR.

Site-directed mutagenesis of *YGR189c*. Plasmid pJV89E, containing the *YGR189c* ORF (Table 2), was used as a template for PCR. Primers were designed to achieve the changes D136N and E138Q. Briefly, two PCRs were run in parallel using the primers A1–A2 and A3–A4 (see Table 1). Both the A1–A2 (442 bp) and A3–A4 (324 bp) PCR products were utilized as overlapping templates in a second PCR with A1 and A4 as external primers. Thus, a final product of 742 bp was generated, corresponding to a mutated internal fragment of the ORF. Finally, a 481-bp *Mam*I/*Spe*I fragment from this PCR product was verified by sequencing and subcloned into *Mam*I/*Spe*I-cleaved pJV89E, thus replacing the wild-type sequence with the mutant sequence.

Confocal-microscopy techniques. Cells were grown overnight in YED (bearing pJV40G) or SD-Ura (bearing pJV89G) and then transferred to fresh medium. After 3 h of incubation, they were harvested by gentle centrifugation, washed twice with phosphate-buffered saline (PBS), and finally resuspended in PBS. For chitin-staining experiments, wheat germ agglutinin-tetramethyl rhodamine isocyanate (WGA-TRITC) (Molecular Probes, Eugene, Oreg.) was used according to the manufacturer's instructions. Samples were observed with an Eclipse TE-300 (Nikon, Tokyo, Japan) microscope attached to a Bio-Rad (Hampstead, United Kingdom) MRC1024 confocal system. Experiments to monitor GFP fusion protein localization over time were performed as above, but samples were mounted on thin SD agar or YED layers, as previously described (20), and time lapse confocal images were taken. When required, cultures were previously synchronized with α-factor (Sigma) as described above.

Cell wall fractionation experiments. To collect cell walls, 100-ml cultures in YED medium were grown to an OD_{600} of 0.8 (approximately 10^7 cells per ml). Cells were washed twice with phosphate buffer, pH 8.5, resuspended in 1 ml of the same buffer, broken in a Fastprep fp120 (Bio 101) with the aid of 1-mm-diameter glass beads according to the manufacturer's instructions (cell breakage was verified by phase-contrast microscopy), and centrifuged. The resulting pellet was washed five times with phosphate buffer, pH 8.5, resuspended in the same buffer containing 0.02% sodium azide, and treated with pronase (Boehringer Mannheim) for 16 h at 35°C with gentle shaking. After centrifugation of this material, the pellet thus obtained was washed twice with phosphate buffer, resuspended in 0.5 ml of the same buffer, heated at 100°C for 10 min, and finally washed again twice. This was considered to be the whole protein-depleted cell wall glucan. To extract the alkali-soluble fraction, this residue was resuspended in 1 ml of 1 M KOH and heated at 60°C for 30 min. The supernatant was then neutralized with acetic acid and precipitated with 2 ml of ethanol. The pellets corresponding to both the soluble and insoluble fractions were washed three times with phosphate buffer. Then the insoluble fraction was resuspended in 1 ml of 0.5 M acetic acid and maintained at 100°C for 3 h in order to extract an alkali-insoluble, acid-soluble fraction. The supernatant was neutralized with KOH, and this fraction was precipitated with 2 ml of ethanol. Both the acid-soluble and -insoluble fractions were washed three times with phosphate buffer. Finally, the pellets of all three (alkali-soluble; alkali-insoluble, acid-soluble; and alkali-insoluble, acid-insoluble) fractions were allowed to dry in a vacuum system, and their dry weights were determined.

Chitin determination in cell walls. Chitin levels were measured as described previously by Kapteyn et al. (24).

RESULTS

The *S. cerevisiae* genome has three ORFs that code for homologous putative glycosidases. In previous studies, the *YGR189c* gene was sequenced (1) and its deletion showed it to be nonessential (40). A search in the databases yielded two predicted protein sequences from the *S. cerevisiae* genome that showed significant degrees of similarity with the deduced *YGR189c* gene product (Fig. 1A): the *YEL040w* (29% identity and 46% similarity in 408 amino acids) and *YLR213c* (34% identity and 49% similarity in 227 amino acids) gene products.

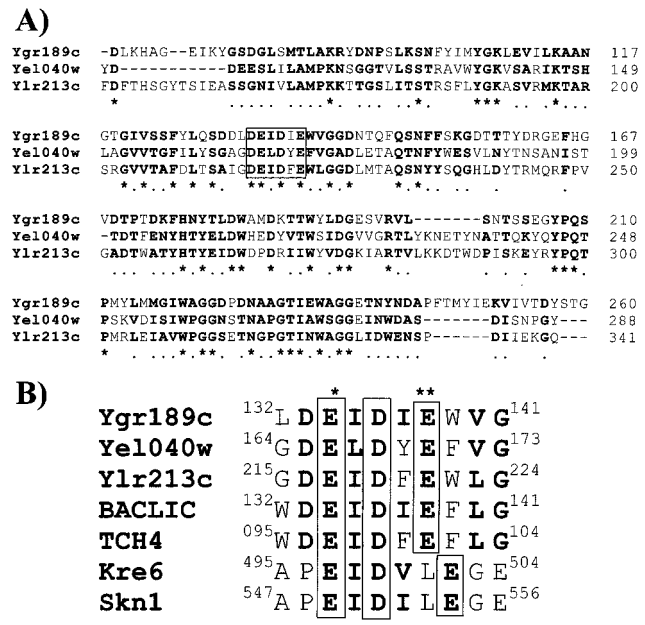

FIG. 1. (A) Amino acid alignment of homologous Ygr189c, Yel040w, and Ylr213c sequences. Identical and conserved residues are boldfaced and are indicated by asterisks and dots, respectively. The putative catalytic domain similar to that of the 1,3-1,4-β-glucanases from *Bacillus licheniformis* is boxed. (B) Amino acid alignment of homologous sequences within the proposed catalytic domain of bacterial endo-β-1,3-1,4-glucanases (48), corresponding to Ygr189c, Yel040w, Ylr213c, Kre6, and Skn1 from *S. cerevisiae*, *B. licheniformis* 1,3-1,4-β-glucanase (BACLIC), and *A. thaliana* xyloglucan endotransglycosidase (TCH4). A single asterisk identifies the proposed catalytic nucleophile (18, 21), and two asterisks indicate the position of the proposed general acid-base residue (49). Amino acids that are identical in all the sequences are boxed. Boldface indicates residues of conserved properties with respect to the *B. licheniformis* domain in more than three sequences. Numbers correspond to the amino acid positions in the protein sequences.

In turn, Ylr213c and Yel040w share 39% identity and 56% similarity along 324 amino acids. All three proteins have an N-terminal secretion signal for their incorporation into the secretory pathway. Furthermore, the proteins encoded by *YGR189c* and *YEL040w*, but not *YLR213c*, also display a potential carboxy-terminal domain for GPI anchor attachment (5, 14), a characteristic of many glycoproteins that are targeted to the cell wall, and a C-terminal Ser- and Thr-rich region, a typical feature of several heavily O-glycosylated cell wall or periplasmic proteins.

Interestingly, Ygr189c, Yel040w, and Ylr213c bear a DE(I/L)DXE motif that is homologous to that included in the proposed catalytic domain of prokaryotic endo-β-1,3-1,4-glucanases (48). A similar motif is found in various xyloglucan endotransglycosidases from plants that also share some similarity with the above-mentioned yeast gene products (Fig. 1B). It has been reported that in bacteria, the first glutamate in this domain may act as the catalytic nucleophile (18, 21) and the second might be the general acid-base residue involved in the double-displacement catalytic mechanism for retaining glycosidases (49); both glutamate residues are essential for the activity of the enzyme. The first glutamate in this motif has also been described to be essential for the activity of the *Arabidopsis thaliana* xyloglucan transglycosidase (4). On the basis of this analysis, Ygr189c, Yel040w, and Ylr213c would belong to a subfamily of yeast glycosidases included in the broad family 16 of glycoside hydrolases within the classification proposed by Henrissat and Bairoch (16; http://afmb.cnrs-mrs.fr/~pedro/CAZY/) that could be involved in cell wall dynamics in the budding yeast. The other two budding-yeast proteins included in this family are Skn1 and Kre6 (similarity to glycosidases from family 16 within the catalytic domain is shown in Fig. 1), two proteins that function in the Golgi apparatus in processes related to β-1,6-glucan synthesis (41), but no significant homology outside the putative catalytic domain was found between the Skn1–Kre6 and Ygr189c–Yel040w–Ylr213c groups.

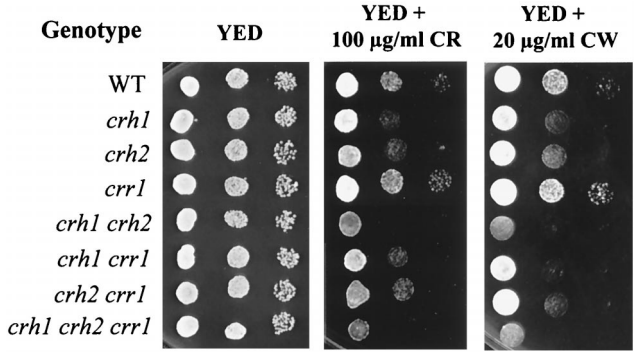

FIG. 2. Sensitivities to Congo red and Calcofluor white of strains bearing all the possible combinations of deletions of the *CRH1*, *CRH2*, and *CRR1* genes. Cells were grown in YED, and 1/10 dilution series of each strain were spotted onto YED plates containing the indicated amounts of Congo red and Calcofluor white.

Deletion of *CRH1*/*YGR189c* and *CRH2*/*YEL040w* causes additive sensitivity to Calcofluor white and Congo red. To explore the roles of *YGR189c*, *YEL040w*, and *YLR213c* in cell wall construction, a search for cell wall-specific phenotypes was carried out on FY1679-derived strains with deletions of these genes. Haploid strains with the *YGR189c* gene deleted had been constructed in the FY1679 background by incorporation of a Kan^r marker (40). *yel040w* and *ylr213c* deletant strains were constructed by replacing the ORF with the *HIS3* and *LEU2* markers, respectively (see Materials and Methods). We found that deletion of either *YGR189c* or *YEL040w* led to sensitivity to the cell wall-binding dyes Calcofluor white and Congo red (Fig. 2), both of which are known to interfere with proper assembly of cell wall components. When spotted onto Congo red and Calcofluor white plates, *ylr213*Δ strains did not show any sensitivity to these compounds (Fig. 2). We shall refer to *YGR189c* and *YEL040w* (previously designated *UTR2*, for transcript with undetermined function [33]) as *CRH1* and *CRH2*, respectively (for Congo red hypersensitive), below. The *YLR213c* gene will be referred to as *CRR1*, for *CRH* related.

The Congo red sensitivities of *crh1*Δ and *crh2*Δ strains were partially or totally complemented by transformation with the wild-type *CRH1* and *CRH2* genes respectively, either in a pRS416-derived centromeric plasmid or in a multicopy plasmid (data not shown).

Interestingly, the strains with deletions of both homologous genes, *CRH1* and *CRH2*, displayed a more-severe Congo red and Calcofluor white sensitivity phenotype than any of the single mutants (Fig. 2). This additive effect might reflect a common function of the two genes in the maintenance of the cell wall architecture. Furthermore, the enhanced sensitivity of the double disruptant to Congo red could be partially alleviated by expression of either of the two genes in centromeric and, more efficiently, in episomic vectors (Fig. 3A). These data indicate a dose-dependent complementation of the *crh1*Δ *crh2*Δ double mutant by either *CRH1* or *CRH2*. Peculiarly, the severe Congo red sensitivity phenotype of double mutants was notably diminished when galactose, instead of glucose, was used as the only carbon source, while this remission was not

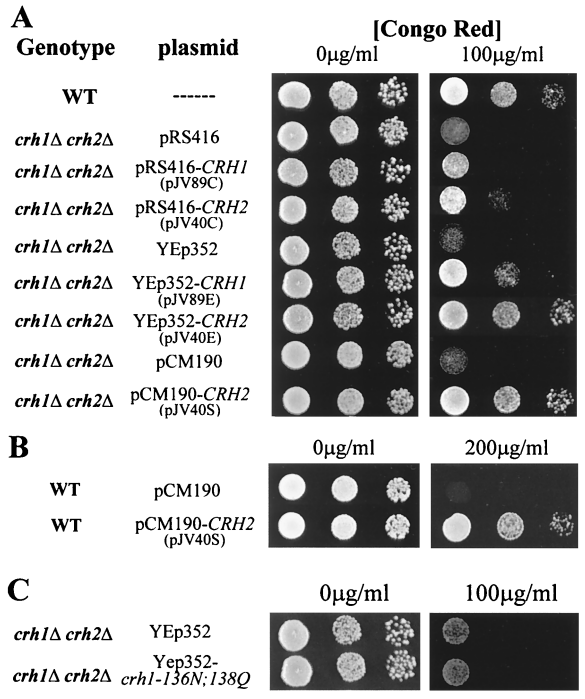

FIG. 3. (A) Complementation studies on a *crh1 crh2* deletion strain growing on YED plates containing Congo red at the amounts indicated and transformed with various plasmids harboring the wild-type (WT) *CRH1* or *CRH2* gene in a pRS416-based centromeric vector, a YEp352-based episomic vector, or the pCM190-based overexpression vector (see Table 2). (B) Resistance to Congo red induced by overexpression of *CRH2* in a wild-type background. (C) A mutant *crh1-136N,138Q* allele does not complement the sensitivity to Congo red in the *crh1*Δ *crh2*Δ strain.

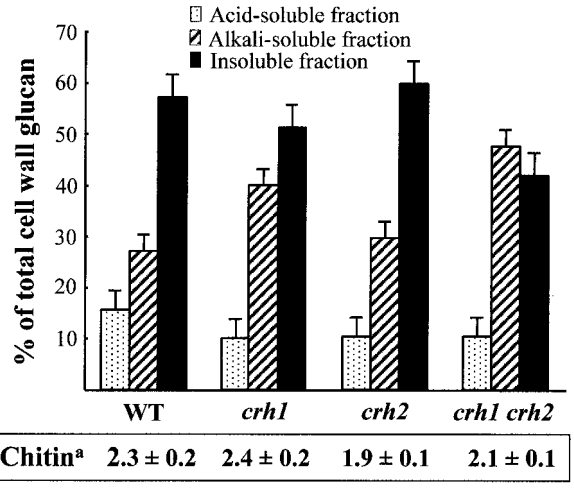

FIG. 4. Determination of the alkali-insoluble–acid-soluble, alkali-soluble, and alkali-insoluble–acid-insoluble fractions of cell wall glucan in wild-type, *crh1*Δ, *crh2*Δ, and *crh1*Δ *crh2*Δ cells. The whole glucan fraction that remained after protease treatment of purified cell walls was considered 100%. [a], the chitin content for each strain, in micrograms of glucosamine per milligram (dry weight) of cells, is given.

observed when a glucose-galactose mixture was used (data not shown).

The introduction of *CRH2*, but not *CRH1*, into an episomic vector in a wild-type background caused enhanced tolerance to Congo red (data not shown). *CRH2* was introduced into the pCM190 plasmid and expressed under the control of a tetracycline-repressible *tetO* promoter that induces high expression of the gene under its control (10). Wild-type cells overexpressing the *CRH2* gene in the absence of doxycycline were able to grow at concentrations of Congo red up to 200 μg/ml, which are highly restrictive for this strain (Fig. 3B).

To determine whether the catalytic activities of these proteins were related to their functions, the putative catalytic DE(I/L)DXE domain described above was mutated and tested for its ability to complement the Congo red sensitivity phenotype. A PCR strategy (see Materials and Methods) was devised that allowed the simultaneous substitution of two amino acids (D at 136 to N and E at 138 to Q) within this motif, the putative acid-base donors previously described as being essential for the catalytic activity of the homologous endo-β-1,3-1,4 glucanases from *Bacillus* spp. (21). The *crh1-136N,138Q* mutant allele was unable to complement the Congo red sensitivity of the *crh1 crh2* double deletant when expressed in a multicopy plasmid (pJV89M) (Fig. 3C), indicating that the integrity of the hypothetical catalytic domain of Crh1 is necessary for the function of this protein.

By genetic means, we generated double *crh1*Δ *crr1*Δ and *crh2*Δ *crr1*Δ strains and triple *crh1*Δ *crh2*Δ *crr1*Δ strains. All combinations were viable. In fact, the deletion of *crr1* did not cause any significant alterations in the phenotype described for single *crh1* or *crh2* deletants or for double *crh1 crh2* deletants when they were analyzed for growth in the presence of Calcofluor white or Congo red (Fig. 2).

Single, double, and triple homozygous deletant diploid strains were generated and found to sporulate with an efficiency comparable to that of the isogenic FY1679 strain, leading us to conclude that these genes are not essential for sporulation under standard laboratory conditions.

The solubility of β-glucan in alkali is altered in *crh1 crh2* mutants. Chemical fractionation of isolated cell walls (7) from wild-type, *crh1*Δ, *crh2*Δ, and *crh1 crh2* double-mutant strains was carried out to detect possible modifications in the distribution of cell wall polymers. Cell walls from various clones of each strain were isolated, digested with pronase to eliminate mannoproteins, and treated with hot alkali to obtain an alkali-soluble fraction. The insoluble residue was subjected to an acid treatment, leading to the isolation of a minor acid-soluble fraction and a residual acid-insoluble, alkali-insoluble fraction. Glucan insolubility in alkali is due to its binding to chitin (15, 26), so variations in the normal proportions of soluble and insoluble β-glucan may reflect either an altered proportion of glucan and chitin in the cell wall or an abnormal degree of cross-linking between these polymers. The average percentage (dry weight) of each fraction obtained from these experiments is shown in Fig. 4; the whole pronase-treated polysaccharide residue is considered 100%. According to these data, the alkali-soluble fraction increased in the *crh1*Δ strain compared to the wild type. In contrast, no significant variations were found in the *crh2*Δ strain. However, simultaneous deletion of *CRH1* and *CRH2* clearly showed a more severe phenotype than that conferred by single disruption of *CRH1*: the alkali-soluble fraction was almost doubled in the *crh1*Δ *crh2*Δ strain compared to that in the wild type, in detriment to the alkali-insoluble fraction. These data prompted us to measure the levels of chitin in these strains. As shown in Fig. 4, no significant variations in the content of chitin were observed that could explain the differences in the level of alkali-soluble glucan between the wild-type strain and the *crh1* or *crh1 crh2* knockout strain.

Transcriptional regulation of the *CRH1*, *CRH2*, and *CRR1* genes. At this point we wished to know how these genes were

regulated at different stages of the yeast life cycle. To achieve this goal, Northern blot hybridization experiments were carried out on total RNA extracted from cells grown under different conditions. Under normal growth conditions, *CRH2* showed a level of expression approximately sixfold higher than that of the *CRH1* gene. By contrast, the *CRR1* transcript was found at very low levels, about 40 times lower than those of the *CRH1* transcript (data not shown). When glucose was replaced by galactose under standard growth conditions, the expression of the *CRH1* gene approximately doubled (Fig. 5A). To investigate whether the deletion of these genes would cause transcriptional activation of any of the other counterparts, we determined the mRNA levels of each gene in single-deletant backgrounds. As expected, the corresponding transcripts were not detected in strains with deletions of these genes (Fig. 5A). Neither the deletion of *CRH1* nor that of *CRH2* led to a significant variation in the expression of the other two genes of the family. However, the expression of *CRH2* was up-regulated in a *crr1*Δ background.

When RNA samples taken from cells incubated under sporulation-inducing conditions for 24 h were analyzed by Northern blotting, the *CRH2* transcript could not be detected in sporulating cells, while *CRH1* was found to be expressed at about the same levels as in the vegetative cycle. However, the expression levels of *CRR1* under these conditions were about ninefold higher in sporulation than in the vegetative cycle (data not shown). These results suggest that the different members of this family of putative glycosidases might function specifically in different developmental programs.

To gain further insight into the transcriptional regulation of these genes and to see whether the involvement of these proteins in cell wall construction was coordinated during the cell cycle, cultures of wild-type FY1679 *MAT***a** cells were synchronized with the mating pheromone α-factor. After 3 h of incubation with mating pheromone, cells displayed the characteristic shmoo morphology. The RNA levels of *CRH1*, *CRH2*, and *CRR1* from α-factor-treated samples were comparable to those of vegetatively growing cells, suggesting that the expression of these genes is not regulated differently in budding and mating. Transcription was analyzed at 20-min intervals after the release from mating pheromone-induced arrest. The mRNA levels of *CRH1* increased four- to fivefold in a period of 20 min, when cells were still unbudded, and then fell sharply to far below the initial levels at 60 min after release, when each cell bore a medium-sized bud, thus showing a well-defined G_1 expression peak. A second M/G_1 peak appeared 80 min after mating pheromone release, when cells showed large buds (Fig. 5B). These results demonstrate a cell cycle-dependent expression of *CRH1*. In contrast, *CRH2* transcript levels were notably constant throughout the cell cycle. *CRR1* was expressed at very low levels during vegetative growth, displaying an increase of almost threefold 60 min after the release from α-factor; this can be attributed to a G_2/M stage of the cell cycle (Fig. 5B). In conclusion, these three genes appear to be subject to different patterns of cell cycle-dependent regulation.

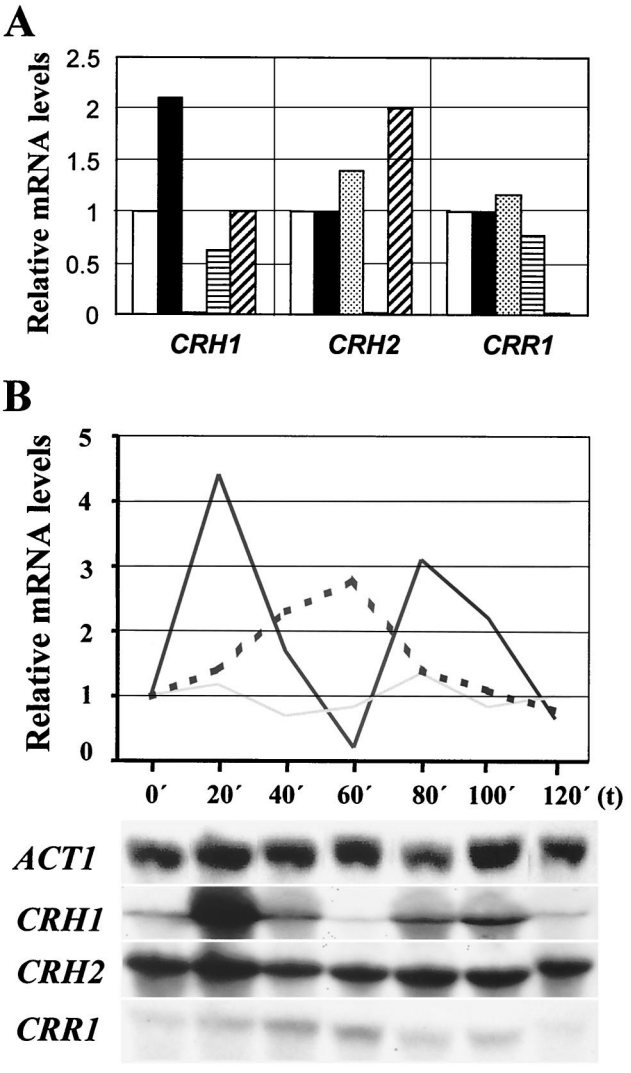

FIG. 5. Northern blot analysis for the study of the expression of the *CRH1*, *CRH2*, and *CRR1* genes. (A) Relative mRNA levels for *CRH1*, *CRH2*, and *CRR1*. mRNA expression levels in a wild-type background when cells were grown in glucose-rich medium (open bars) were assigned a value of 1 for each hybridization assay. The amount of RNA was normalized to that of *ACT1* mRNA (a constitutively expressed gene in *S. cerevisiae*). mRNA levels for each gene in a wild-type background when cells were grown in galactose-based YEG medium (solid bars), in a *crh1*Δ strain grown in YED (stippled bars), in a *crh2*Δ background (horizontally striped bars), and in a *crr1*Δ strain (diagonally striped bars) are also shown. (B) Northern blot analysis of *CRH1*, *CRH2*, and *CRR1* expression during the cell cycle in synchronized haploid cells after release from pheromone-induced arrest (see Materials and Methods). A relative value of 1 was assigned to RNA levels for each transcript at time 0. The exposure times for each film were as follows: 2 h for *ACT1*, overnight for *CRH1* and *CRH2*, and 10 days for *CRR1*. Solid line, *CRH1*; shaded line, *CRH2*; dashed line, *CRR1*.

Crh1- and Crh2-GFP fusions localize at chitin-rich points of the cell wall under different developmental conditions. With a view to determining the subcellular localization of the Crh1 and Crh2 polypeptides in vivo, we constructed plasmids encoding Crh1-GFP and Crh2-GFP fusion proteins. The GFP-coding sequence was cloned into the ORFs of the *CRH1* and *CRH2* genes without altering either the N-terminal secretion signal or the GPI attachment site (see Materials and Methods). Transcription of both GFP fusions was driven by their own gene promoters. *crh1*Δ and *crh2*Δ strains harboring episomic plasmids including GFP fusions were obtained, and fluorescence was followed by confocal microscopy.

Time lapse confocal microscopy allowed the study of the spatial localization of Crh1-GFP in the cell cycle (Fig. 6A through F). A fluorescent patch appeared at the bud site on the cell surface of the mother cell shortly before bud emergence (Fig. 6A) and in cells with an emerging bud (Fig. 6C), but fluorescence was no longer observed at this point in cells with small to medium-sized buds (Fig. 6B and D). However, the protein appeared again at a more advanced stage of the cell

cycle, when the bud reached a large size, at the mother-daughter constriction, marking the cytokinesis plane (Fig. 6E), and remained there even after cell separation had been achieved, marking the bud scar of the mother cell (Fig. 6F). This localization pattern is similar to that of Chs3p (44) and suggests a specific function of Crh1 at a stage prior to bud emergence in late G_1 and probably during cytokinesis. It is also consistent with its cell cycle-dependent transcription pattern (see above).

To monitor the localization and temporal distribution of Crh2p in the cell cycle, haploid *crh2* deletant strains expressing the Crh2-GFP fusion protein were grown on agar microlayers and analyzed by time lapse confocal microscopy. The Crh2p-GFP fusion protein marked the cell surface at all stages of the cell cycle, in accordance with its transcriptional regulation. It was preferentially visualized around the neck area in prebudding cells (Fig. 6H). As the bud grew, Crh2p-GFP appeared as a conspicuous ring at the base of the bud neck (Fig. 6I through M), reminiscent of the prevalent localization of chitin at this stage of the cell cycle. The protein accumulated strongly in the septum area between the mother and daughter cells during the cytokinesis stage (Fig. 6N through O). Crh2p was also found in the lateral cell wall, especially in daughter cells during late stages of the cell cycle (Fig. 6N through O). Finally, the protein marked the preceding division site, especially in the mother cell (bud scar) (Fig. 6P through Q). Observation of confocal sections of cells expressing Crh2-GFP during late stages of the cell cycle and stained with WGA-TRITC, which specifically binds chitin, revealed that Crh2-GFP colocalizes with chitin at the bud neck, defining a Crh2-GFP-rich region encircled by the chitin ring during the cytokinesis stage (Fig. 6R through W). Both in diploid strains with a bipolar budding pattern (Fig. 6X) and in axial-budding haploid strains (Fig. 6Y), chitin and Crh2-GFP colocalized at the bud scar that remains in the mother cell at the site of cytokinesis. Although it rendered a lower intensity of fluorescence, Crh1-GFP was also found to colocalize with chitin at the cytokinetic scar (Fig. 6Z). Localization of Crh2p in cells undergoing mating and expressing Crh2-GFP showed that this protein was concentrated in mating projections (Fig. 6a and b), disappeared after cell fusion (Fig. 6c), and later accumulated in large amounts at the neck of the newly created cell in developing zygotes (Fig. 6d). When diploid cells derived from these zygotes were monitored, the above-described distribution of Crh2p in large-budded cells at the septum between mother and daughter cells and at bipolar bud scars marking the last division was observed (Fig. 6e). However, no fluorescence could be detected when Crh1-GFP-transformed strains were mated under the same conditions. In diploid strains transformed with these fusions and forced to undergo sporulation, Crh1-GFP marked the spore envelopes, sometimes concentrated in intense patches (Fig. 6G). This was not observed in Crh2p-GFP-bearing strains (data not shown).

In view of the localization of Crh1 and Crh2 in chitin-rich areas of the cell surface, we were prompted to test whether there might be any genetic interaction with known chitin synthase genes or whether this localization pattern could be altered in cells depleted of chitin synthase II (CSII) or chitin synthase III (CSIII) activity. CSII is responsible for the synthesis of the primary septum during cytokinesis, and its activity depends on the *CHS2* gene product (45, 47), while CSIII, which is encoded by the *CHS3* gene, is responsible for the bulk of chitin in the cell wall and, especially, that of the neck ring (45). Using classic yeast genetics, we developed strains bearing combinations of *crh1*, *crh2*, and *crr1* deletions and either *chs2* or *chs3* disruptions. The resulting *crh1*Δ *crh2*Δ *chs2*::*LEU2*, *crh1*Δ *crh2*Δ *crr1*Δ *chs2*::*LEU2*, *crh1*Δ *crh2*Δ *chs3*::*LEU2*, and *crh1*Δ *crh2*Δ *crr1*Δ *chs3*::*LEU2* strains were viable, and their phenotype was indistinguishable from those of single *chs2* or *chs3* disruptants. When transformed into chitin synthase (CSII or CSIII)-defective strains, the Crh1p-GFP and Crh2p-GFP fusion proteins localized in the cell wall as described above, showing that cell wall localization is independent of chitin synthesis (data not shown). Nevertheless, *chs2* mutants displayed an enhanced accumulation of Crh2-GFP in the cell wall, especially at the septum area (Fig. 6f).

DISCUSSION

A novel family of yeast cell wall-related proteins. Our knowledge of the yeast cell wall has increased in the past few years. Some of the linkages between yeast cell wall polymers (β-1,3-glucan, β-1,6-glucan, chitin, and mannoproteins) have been described (23, 26, 27), but little is known about the involvement of particular enzymes in the cross-linking mechanisms. Proteins such as Bgl2 or Gas1 have been postulated to exert such a function (13, 37), but no molecular evidence has been provided that such a role is exerted in vivo. To date, the only yeast cell wall enzyme for which a glycosyltransferase activity has been biochemically characterized is Bgl2. This protein was found to function as a β-1,3-glucanosyl transferase (13), although it had previously been described as an exo- (25) and endo-β-1,3-glucanase (35). Here we present a family of homologous yeast cell wall-related proteins, namely, Crh1, Crh2, and Crr1. They show a potential N-terminal signal peptide for their integration into the secretory pathway, and, in addition, Crh1 and Crh2 display in their sequences a C-terminal consensus for GPI anchoring and Ser- and Thr-rich areas, both features characteristic of cell wall proteins (5). In a previous systematic analysis, Hamada et al. (14) have shown the functionality of the GPI-anchoring sequence present in both Crh1 and Crh2 proteins. By means of fusion of the C-terminal domain of each protein to a reporter protein including a secretion signal, α-galactosidase, and a hemagglutinin (HA) epitope, these authors showed that Ygr189c (Crh1) and Yel040w (Crh2) fusion proteins were incorporated into the cell wall and released after treatment with laminarinase (14). These data indicate that Crh1 and Crh2 are cell wall proteins covalently attached to the cell wall glucan. Outside the Ser- and Thr-rich regions, all three proteins show significant similarities to bacterial endo-β-1,3-1,4-glycosidases and plant xyloglucan endotransglycosidases, including a hypothetical catalytic domain. This domain has been perfectly characterized in bacterial endo-β-1,3-1,4-glycosidases, in which glutamates at positions 134 and 138 has been demonstrated to act as a nucleophile and a general acid-base residue, respectively, in the double-displacement catalytic mechanism for retaining glycosidases (49). In the context of the yeast cell wall, where polysaccharide contents are high, it is likely that proteins with putative glycosidase activity (like Crh1, Crh2, and Crr1) would function as glucanosyl transferases. In plants, endotransglycosidase activity has been theorized to participate in cell wall expansion during growth by cutting and rejoining xyloglucan chains that cross-link microfibrils of cellulose in the primary cell wall (9). If it is assumed that this sort of cell wall-biosynthetic mechanism might also work in the yeast cell (3), members of the Crh family could be involved in cross-linking between cell wall polymers by means of transglycosylation reactions.

Strains with either *CRH1* or *CRH2* deleted show sensitivity to Calcofluor white and Congo red, while double *crh1*Δ *crh2*Δ strains display a phenotype of additive sensitivity to these compounds. A large variety of mutants with compromised cell walls have been shown to display enhanced sensitivity to these cell wall-interacting fluorochromes (30, 34, 39), probably because

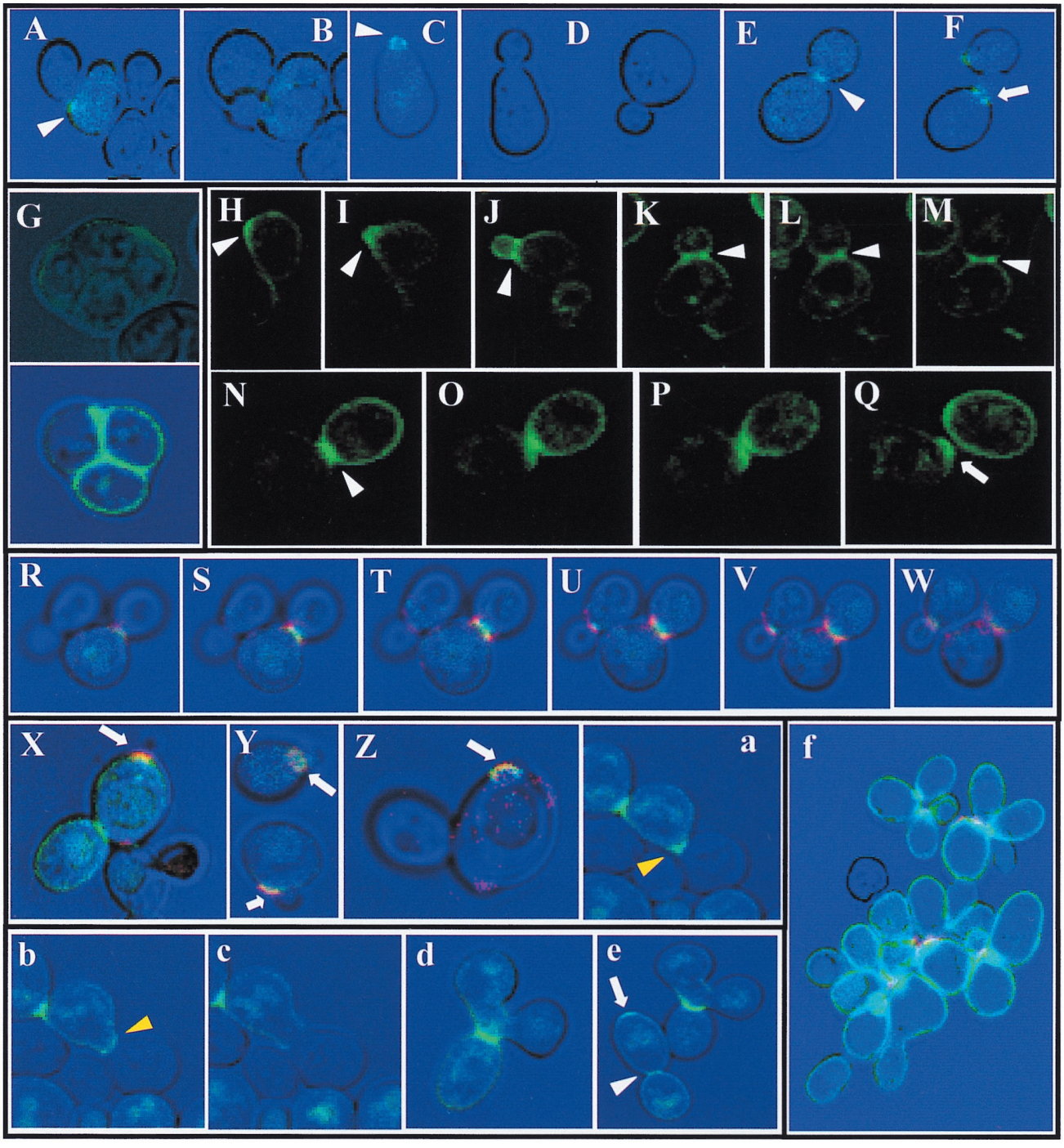

FIG. 6. Cellular localization by confocal microscopy of Crh1-GFP and Crh2-GFP. (A through F) Crh1-GFP visualized in *crh1* cells bearing the pJV89G plasmid during vegetative growth. (A and B) Images of the same cells 45 min apart. The fluorescent patch in panel A marks the site of bud emergence. (C through F) Cells from the same transformant after release from mating pheromone-induced arrest in different stages of the budding cycle: cells with incipient budding (C), with medium-sized buds (D), with large buds (E), and after separation (F). (G) A double homozygous *crh1 crh2* diploid strain transformed with pJV89G and allowed to sporulate, showing Crh1-GFP localization in ascospores. (H through Q) Time lapse localization of Crh2-GFP in *crh2*-deleted cells bearing the pJV40G plasmid. The pictures show a sequence of images taken every 10 min on a growing bud from the stage of bud emergence (H and I), every 20 min during bud growth (J through M), and during the stages of cytokinesis and cell separation at intervals of 10 min, except for the last one (30 min) (N through Q). (R through W) Confocal analysis of six slides (0.5-μm width) of budding cells expressing Chr2-GFP. Red color, chitin-rich areas detected by WGA-TRITC staining; green color, localization of the protein. (X through Y) Colocalization of Crh2-GFP and WGA-TRITC-stained chitin at the bud scar that remains from the last cytokinetic event in both diploid (X) and haploid (Y) backgrounds. (Z) Colocalization of Crh1-GFP and WGA-TRITC-stained chitin at the bud scar. (a through e) *crh2*Δ strain transformed with pJV40G in the process of mating to untransformed cells of the opposite mating type. The sequence in panels a through c shows the localization of Crh2-GFP in the mating projection and throughout the process of cell fusion (time lapse between pictures, 15 min). In panel d, a mature zygote is shown, with Crh2p marking the cytokinesis site. The image in panel e depicts the same zygote after 90 min, when it had developed a second diploid bud. A residual Crh2-GFP mark is apparent at the birth site of the first diploid, showing the bipolar polarity pattern characteristic of diploids. (f) Localization of Crh2-GFP in a *chs2*::*LEU2 crh2*Δ background. White arrowheads indicate accumulation of GFP fusion proteins at incipient bud sites and bud necks. Yellow arrowheads indicate accumulation of fluorescence at the shmoo. Arrows point to GFP-Crh localization at bud scars.

cells with weakened cell walls might not be able to withstand the additional disturbance caused by these drugs (28, 42). The fact that the Congo red sensitivity phenotype of *crh1* and *crh2* mutants is cumulative suggests that the two proteins might exert a common function related to cell wall dynamics.

Analysis of cell walls from wild-type, single *crh1* deletant, and double *crh1 crh2* deletant strains revealed variations in the distribution of alkali-soluble and -insoluble glucan fractions that should reflect in vivo alterations in cell wall architecture. Such alterations are not essential for cell wall integrity or viability and cannot feasibly account for serious alterations in the glucan/chitin or β-1,6-glucan/β-1,3-glucan ratios, since this would be expected to cause characteristic phenotypes that we were unable to detect in Crh-deficient cells. Variations in the proportions of soluble and insoluble glucan may reflect either altered amounts of glucan and chitin in the cell wall or an abnormal degree of cross-linking between these polymers. Reduced levels of either β-1,6- or β-1,3-glucan should cause resistance to K1 or K9 killer toxins, respectively, but none of these phenotypes was exhibited by these mutants (Rodriguez-Peña et al., unpublished data). Moreover, the levels of chitin in the *crh* knockouts do not vary meaningfully compared to those in the wild-type strain. Taking all these data together, the increase in the ratio of alkali-soluble to alkali-insoluble glucan should be expressed in terms of a decrease in the degree of cross-linking among the different cell wall polymers and suggests a role for Crh1 and Crh2 in this process. *CRH2* seems to have a less significant role, since deletion of this gene has little effect or at least can be compensated for in the presence of *CRH1*. However, deletion of *CRH2* leads to an increase in the soluble fraction in the absence of *CRH1*, as shown by the fact that the *crh1 crh2* double mutant phenotype is more severe than the *crh1* defect alone. Taking into account that the alkali insolubility of cell wall glucan is due to its covalent binding to chitin (15, 26, 27), an attractive hypothesis is that in *crh1*Δ *crh2*Δ mutants the β-1,4-linkages between chitin and β-1,3-glucan would be reduced, leading to the detected increase in the alkali-soluble glucan fraction. Another possibility is that these genes are involved in β-1,3-glucan branching. Thus, in their absence there would be less availability of reducing ends to which other cell wall components, such as chitin, could be attached. Without a characterized enzymatic activity for these proteins, an important finding is that an allele that encodes a Crh1-136N,138Q mutant protein, with an impaired hypothetical catalytic domain, is unable to complement a Crh^- phenotype, suggesting a critical role for these putative catalytic residues in the function of the protein.

***CRH1*, *CRH2*, and *CRR1* are regulated differently during the yeast life cycle.** The fact that the cell wall is a dynamic structure in the different developmental programs of the yeast life cycle implies that the biosynthesis and assembly of cell wall components must be accurately regulated. Although Crh1 and Crh2 might have an overlapping function, their different patterns of expression and protein localization suggest a specific role for each protein of the family in different stages of the yeast life cycle. While *CRH2* transcript levels are high and stable throughout the mitotic cycle, *CRH1* expression is less abundant but reaches two maximum points: a clear G_1 peak and a second peak at M/G_1. The late G_1 phase is associated with early stages of budding, a crucial point in the construction of the cell wall, which has to be remodeled for bud emergence and growth. Consistent with this, several proteins involved in the biosynthesis of cell wall components and cell wall construction, among which are *FKS1*, *KRE6*, *CSD2*, and *GAS1*, have been shown to be specifically expressed at this stage (19). Probably, periodic expression of genes involved in cell wall construction helps the cell to successfully pass through this stage (19).

The *CRR1* transcript is very weakly expressed in the mitotic cycle. However, it appears to peak at G_2/M, a behavior that clearly differs from that of *CRH1*. Both the *CRH1* and *CRR1* genes are expressed in sporulating cells, and the expression of *CRR1* is especially significant under these conditions. While Crh1 might therefore function both in the mitotic and meiotic cycles, it is very likely that Crr1 is mainly involved in sporulation, in view of the low transcript levels detected in vegetative growth. Nevertheless, elimination of the *CRR1* gene caused enhanced expression of *CRH2* in the mitotic cycle, suggesting that Crr1 may also play a role in bud development—which would explain its G_2/M expression peak—that could be counterbalanced by its homolog.

Crh1 and Crh2 localize at polarized growth sites. Here we provide evidence that both Crh1 and Crh2 are localized at the cell surface. To our knowledge, this is the first time that a detailed localization pattern has been reported for a cell wall protein by means of fusion to GFP under different developmental conditions. In general, the localization of these proteins is reminiscent of the distribution of cell wall chitin, which is mainly concentrated in the ring at the bud neck and the subsequent bud scar. Nevertheless, the distribution and timing of Crh1- and Crh2-GFP fusion proteins during the mitotic cycle revealed differences between them, consistent with their different transcription profiles and with the possibility of these two genes performing their common function at different cell cycle stages. Crh1-GFP is located at the site of bud emergence and, later, at the mother-daughter constriction in large-budded cells, consistent with the peaking of *CRH1* transcripts at the equivalent cell cycle stages. On the other hand, the expression of the *CRH2* gene did not vary significantly during the cell cycle, and consequently Crh2-GFP was detectable throughout the entire budding process. Crh2-GFP was concentrated at the chitin-rich bud neck, although it was also detectable throughout the lateral cell wall. At the time of cell separation, the Crh2-GFP signal in the lateral wall was more conspicuous in the daughter than in the mother cell. Interestingly, chitin has been reported to be absent from the lateral walls of daughter cells until the time of septum formation (45). Moreover, both Crh1- and Crh2-GFP fusion proteins frequently marked the bud scar remaining from the previous budding event, but not older scars, as determined by simultaneous staining of chitin with rhodamine-conjugated WGA. It has been shown by others that the chitin participating in the linkages to both β-1,3- and β-1,6-glucan is synthesized by CSIII (26, 27). This chitin is found at the base of an emerging bud and, in a dispersed form, is interspersed through the whole cell wall. On the basis of Crh1 localization, a suggestive hypothesis might be the involvement of this protein in glucan-chitin assembly early at the budding site and later at the septum formed between mother and daughter cells at cytokinesis. In the case of Crh2, its timing and localization indicate a role for this protein in assembly during the whole budding process, not only at the neck but also in the lateral cell wall.

We report that Crh1 and Crh2 localization is maintained in both *chs2* and *chs3* mutants. *CHS2* and *CHS3* are responsible for chitin deposition at the primary septum and the chitin ring at the bud neck, respectively (45, 47). This should mean that localization of Crh1 and Crh2 does not depend on chitin deposition. It has been reported that *chs2* mutants display aberrantly thick septa very rich in chitin (45). The enhanced signal of Crh2p-GFP both in lateral cell walls and in thickened septa in *chs2* mutants strongly suggests that the presence of this

protein on the cell surface depends on the mechanisms that compensate for the loss of CSII activity.

Two events are involved in bud growth: (i) an increased synthesis and assembly of cell wall components and (ii) polarization of growth by rearrangement of the cytoskeleton and the secretory machinery to specifically deliver the cell wall constituents to the bud (19). Thus far, a considerable array of yeast proteins have been localized at polarized growth sites (31), most of them functioning to support polarized secretion for the growth of the cell surface. Some of these proteins, such as Chs3, are important for cell wall construction itself. In fact, Chs3 presents timing and localization very similar to those of Crh1 (44), and such a distribution has been shown to depend on a complex in which Chs4, Bni4, and septins are involved (6). Our findings raise the possibility that the mechanisms for establishing polarity might affect proteins such as Crh1 and Crh2 that are localized extracytoplasmically. The subcellular distribution of these proteins is consistent with the idea that they might play a role in cell wall assembly at the sites of polarized growth.

In the context of our current knowledge of the cell wall, our results define a new family of proteins clearly involved in cell wall polymer assembly and the remodeling of this cell structure. Supporting this, it has recently been reported that the expression levels of *CRH1*, together with other genes encoding proteins involved in cell wall construction and maintenance, are significantly increased in response to activation of the Slt2/Mpk1 cell integrity signaling pathway (22).

The differential cell cycle-dependent regulation and localization of these proteins suggest that their functions might be required in different stages of the life cycle, namely, at bud emergence, cytokinesis, and sporulation for Crh1 and throughout the whole budding cycle and mating process for Crh2. In contrast, Crr1 seems to play its main role under sporulating conditions.

ACKNOWLEDGMENTS

We thank Enrique Herrero for providing us with the pCM190 overexpression plasmid, A. Durán for providing strains, P. de Groot, F. Klis, M. Molina, and M. Sánchez for useful discussions and help, M. Isabel García-Sáez and Rosa Pérez of the Centro de Secuenciación Automatizada de DNA (Universidad Complutense) for oligonucleotide synthesis and sequencing, and A. Alvárez of the Centro de Citometría y Microscopía Confocal (Universidad Complutense) for expert help in confocal microscopy.

This work was supported by the Commission of the European Union within the EUROFAN I (BIO4-CT95-0080) and EUROFAN II (BIO4-CT97-2294) programs and cofinanced by the Spanish Comisión Interministerial de Ciencia y Tecnología (Project BIO97-1570-CE). J.M.R.-P. was aided by a postdoctoral fellowship from the Consejería de Educación y Cultura, Comunidad de Madrid, Spain.

REFERENCES

1. **Arroyo, J., M. Garcia-Gonzalez, M. I. Garcia-Saez, M. Sanchez, and C. Nombela.** 1997. DNA sequence analysis of a 23,002 bp DNA fragment of the right arm of *Saccharomyces cerevisiae* chromosome VII. Yeast **13:**357–363.
2. **Ausubel, F. M., R. Brent, R. E. Kingston, D. D. Moore, J. G. Seidman, J. A. Smith, and K. Struhl.** 1993. Current protocols in molecular biology. Greene Publishing Associates and Wiley Interscience, New York, N.Y.
3. **Cabib, E., R. Roberts, and B. Bowers.** 1982. Synthesis of the yeast cell wall and its regulation. Annu. Rev. Biochem. **51:**763–793.
4. **Campbell, P., and J. Braam.** 1998. Co- and/or post-translational modifications are critical for TCH4 XET activity. Plant J. **15:**553–561.
5. **Caro, L. H. P., H. Tettelin, J. H. Vossen, A. F. J. Ram, H. Van Den Ende, and F. M. Klis.** 1997. *In silicio* identification of glycosyl-phosphatidylinositol-anchored plasma-membrane and cell wall proteins of *Saccharomyces cerevisiae*. Yeast **13:**1477–1489.
6. **DeMarini, D. J., A. E. M. Adams, H. Fares, C. De Virgilio, G. Valle, J. S. Chuang, and J. R. Pringle.** 1997. A septin-based hierarchy of proteins required for localized deposition of chitin in the *Saccharomyces cerevisiae* cell wall. J. Cell Biol. **139:**75–93.
7. **Fleet, G. H.** 1991. Cell walls, p. 199–277. *In* A. H. Rose and J. S. Harrison (ed.), The yeasts. Academic Press, New York, N.Y.
8. **Fleet, G. H., and D. J. Manners.** 1976. Isolation and composition of an alkali-soluble glucan from the cell walls of *Saccharomyces cerevisiae*. J. Gen. Microbiol. **94:**180–192.
9. **Fry, S. C., R. C. Smith, K. F. Renwick, D. J. Martin, S. K. Hodge, and K. J. Matthews.** 1992. Xyloglucan endotransglycosylase, a new wall-loosening enzyme activity from plants. Biochem. J. **282:**821–828.
10. **Gari, E., L. Piedrafita, M. Aldea, and E. Herrero.** 1997. A set of vectors with a tetracycline-regulatable promoter system for modulated gene expression in *Saccharomyces cerevisiae*. Yeast **13:**837–848.
11. **Gietz, R. D., and A. Sugino.** 1988. New yeast-*Escherichia coli* shuttle vectors constructed with in vitro mutagenized yeast genes lacking six-base pair restriction sites. Gene **74:**527–534.
12. **Gietz, R. D., and R. A. Woods.** 1994. High efficiency transformation with lithium acetate, p. 121–134. *In* J. R. Johnston (ed.), Molecular genetics of yeast: a practical approach. IRL Press, Oxford, United Kingdom.
13. **Goldman, R. C., P. A. Sullivan, D. Zakula, and J. O. Capobianco.** 1995. Kinetics of β-1,3 glucan interaction at the donor and acceptor sites of the fungal glucosyltransferase encoded by the *BGL2* gene. Eur. J. Biochem. **227:**372–378.
14. **Hamada, K., S. Fukuchi, M. Arisawa, M. Baba, and K. Kitada.** 1998. Screening for glycosylphosphatidylinositol (GPI)-dependent cell wall proteins in *Saccharomyces cerevisiae*. Mol. Gen. Genet. **258:**53–59.
15. **Hartland, R. P., C. A. Vermeulen, F. M. Klis, J. H. Sietsma, and J. G. Wessels.** 1994. The linkage of (1-3)-β-glucan to chitin during cell wall assembly in *Saccharomyces cerevisiae*. Yeast **10:**1591–1599.
16. **Henrissat, B., and A. Bairoch.** 1996. Updating the sequence-based classification of glycosyl hydrolases. Biochem. J. **316:**695–696.
17. **Hill, J. E., A. M. Myers, T. J. Koerner, and A. Tzagoloff.** 1986. Yeast/*E. coli* shuttle vectors with multiple unique restriction sites. Yeast **2:**163–167.
18. **Hoj, P. B., R. Condron, J. C. Traeger, J. C. McAuliffe, and B. A. Stone.** 1992. Identification of glutamic acid 105 at the active site of *Bacillus amyloliquefaciens* 1,3-1,4-β-D-glucan 4-glucanohydrolase using epoxide-based inhibitors. J. Biol. Chem. **267:**25059–25066.
19. **Igual, J. C., A. L. Johnson, and L. H. Johnston.** 1996. Coordinated regulation of gene expression by the cell cycle transcription factor SWI4 and the protein kinase C MAP kinase pathway for yeast cell integrity. EMBO J. **15:**5001–5013.
20. **Jimenez, J., V. J. Cid, R. Cenamor, M. Yuste, G. Molero, C. Nombela, and M. Sanchez.** 1998. Morphogenesis beyond cytokinetic arrest in *Saccharomyces cerevisiae*. J. Cell Biol. **143:**1617–1634.
21. **Juncosa, M., J. Pons, T. Dot, E. Querol, and A. Planas.** 1994. Identification of active site carboxylic residues in *Bacillus licheniformis* 1,3-1,4-β-D-glucan 4-glucanohydrolase by site-directed mutagenesis. J. Biol. Chem. **269:**14530–14535.
22. **Jung, U. S., and D. E. Levin.** 1999. Genome-wide analysis of gene expression regulated by the yeast cell wall integrity signalling pathway. Mol. Microbiol. **34:**1049–1057.
23. **Kapteyn, J. C., H. Van Den Ende, and F. M. Klis.** 1999. The contribution of cell wall proteins to the organization of the yeast cell wall. Biochim. Biophys. Acta **1426:**373–383.
24. **Kapteyn, J. C., P. Van Egmond, E. Sievi, H. Van Den Ende, M. Makarow, and F. M. Klis.** 1999. The contribution of the O-glycosylated protein Pir2p/Hsp150 to the construction of the yeast cell wall in wild-type cells and β-1,6-glucan-deficient mutants. Mol. Microbiol. **31:**1835–1844.
25. **Klebl, F., and W. Tanner.** 1989. Molecular cloning of a cell wall exo-β-1,3-glucanase from *Saccharomyces cerevisiae*. J. Bacteriol. **171:**6259–6264.
26. **Kollár, R., E. Petráková, G. Ashwell, P. W. Robbins, and E. Cabib.** 1995. Architecture of the yeast cell wall. The linkage between chitin and β(1→3)-glucan. J. Biol. Chem. **270:**1170–1178.
27. **Kollár, R., B. B. Reinhold, E. Petráková, H. J. C. Yeh, G. Ashwell, J. Drgonová, J. C. Kapteyn, F. M. Klis, and E. Cabib.** 1997. Architecture of the yeast cell wall. β(1→6)-Glucan interconnects mannoprotein, β(1→)3-glucan, and chitin. J. Biol. Chem. **272:**17762–17775.
28. **Kopecka, M., and M. Gabriel.** 1992. The influence of Congo red on the cell wall and (1-3)-β-D-glucan microfibril biogenesis in *Saccharomyces cerevisiae*. Arch. Microbiol. **158:**115–126.
29. **Lipke, P. N., and R. Ovalle.** 1998. Cell wall architecture in yeast: new structure and new challenges. J. Bacteriol. **180:**3735–3740.
30. **Lussier, M., A.-M. White, J. Sheraton, T. Di Paolo, J. Treadwell, S. B. Southard, C. I. Horenstein, J. Chen-Weiner, A. F. J. Ram, J. C. Kapteyn, T. W. Roemer, D. H. Vo, D. C. Bondoc, J. Hall, W. W. Zhong, A.-M. Sdicu, J. Davies, F. M. Klis, P. W. Robbins, and H. Bussey.** 1997. Large scale identification of genes involved in cell surface biosynthesis and architecture in *Saccharomyces cerevisiae*. Genetics **147:**435–450.
31. **Madden, K., and M. Snyder.** 1998. Cell polarity and morphogenesis in budding yeast. Annu. Rev. Microbiol. **52:**687–744.
32. **McKnight, G. L., T. S. Cardillo, and F. Sherman.** 1981. An extensive deletion causing overproduction of yeast iso-2-cytochrome *c*. Cell **25:**409–419.
33. **Melnick, L., and F. Sherman.** 1993. The gene clusters ARC and COR on chromosomes 5 and 10, respectively, of *Saccharomyces cerevisiae* share a

common ancestry. J. Mol. Biol. **233:**372–388.
34. **Moukadiri, I., J. Armero, A. Abad, R. Sentandreu, and J. Zueco.** 1997. Identification of a mannoprotein present in the inner layer of the cell wall of *Saccharomyces cerevisiae*. J. Bacteriol. **179:**2154–2162.
35. **Mrsa, V., F. Klebl, and W. Tanner.** 1993. Purification and characterization of the *Saccharomyces cerevisiae BGL2* gene product, a cell wall endo-β-1,3-glucanase. J. Bacteriol. **175:**2102–2106.
36. **Orlean, P.** 1997. Biogenesis of yeast wall and surface components, p. 229–362. *In* J. Pringle, J. Broach, and E. Jones (ed.), Molecular and cellular biology of the yeast *Saccharomyces*. Cold Spring Harbor Laboratory Press, Cold Spring Harbor, N.Y.
37. **Popolo, L., and M. Vai.** 1999. The Gas1 glycoprotein, a putative wall polymer cross-linker. Biochim. Biophys. Acta **1426:**385–400.
38. **Pringle, J. R.** 1991. Staining of bud scars and other cell wall chitin with Calcofluor. Methods Enzymol. **194:**732–735.
39. **Ram, A. F. J., A. Wolters, R. Ten Hoopen, and F. M. Klis.** 1994. A new approach for isolating cell wall mutants in *Saccharomyces cerevisiae* by screening for hypersensitivity to Calcofluor White. Yeast **10:**1019–1030.
40. **Rodriguez-Peña, J. M., V. J. Cid, M. Sanchez, M. Molina, J. Arroyo, and C. Nombela.** 1998. The deletion of six ORFs of unknown function from *Saccharomyces cerevisiae* chromosome VII reveals two essential genes: *YGR195w* and *YGR198w*. Yeast **14:**853–860.
41. **Roemer, T., G. Paravicini, M. A. Payton, and H. Bussey.** 1994. Characterization of the yeast (1→6)-β-glucan biosynthetic components, Kre6p and Skn1p, and genetic interactions between the *PKC1* pathway and extracellular matrix assembly. J. Cell Biol. **127:**567–579.
42. **Roncero, C., and A. Duran.** 1985. Effect of Calcofluor White and Congo red on fungal cell wall morphogenesis: in vivo activation of chitin polymerization. J. Bacteriol. **163:**1180–1185.
43. **Sambrook, J., E. F. Fritsch, and T. Maniatis.** 1989. Molecular cloning: a laboratory manual. Cold Spring Harbor Laboratory, Cold Spring Harbor, N.Y.
44. **Santos, B., and M. Snyder.** 1997. Targeting of chitin synthase 3 to polarized growth sites in yeast requires Chs5p and Myo2p. J. Cell Biol. **136:**95–110.
45. **Shaw, J. A., P. C. Mol, B. Bowers, S. J. Silverman, M. H. Valdivieso, A. Duran, and E. Cabib.** 1991. The function of chitin synthases 2 and 3 in the *Saccharomyces cerevisiae* cell cycle. J. Cell Biol. **114:**111–123.
46. **Sikorski, R. S., and P. Hieter.** 1989. A system of shuttle vectors and yeast host strains designed for efficient manipulation of DNA in *Saccharomyces cerevisiae*. Genetics **122:**19–27.
47. **Silverman, S. J., A. Sburlati, M. L. Slater, and E. Cabib.** 1988. Chitin synthase 2 is essential for septum formation and cell division in *Saccharomyces cerevisiae*. Proc. Natl. Acad. Sci. USA **85:**4735–4739.
48. **Tabernero, C., P. M. Coll, J. M. Fernandez-Abalos, P. Perez, and R. I. Santamaria.** 1994. Cloning and DNA sequencing of *bgaA*, a gene encoding an endo-β-1,3-1,4-glucanase, from an alkalophilic *Bacillus* strain (N137). Appl. Environ. Microbiol. **60:**1213–1220.
49. **Viladot, J. L., E. de Ramon, O. Durany, and A. Planas.** 1998. Probing the mechanism of *Bacillus* 1,3-1,4-β-D-glucan 4-glucanohydrolases by chemical rescue of inactive mutants at catalytically essential residues. Biochemistry **37:**11332–11342.
50. **Wach, A., A. Brachat, C. Alberti-Segui, C. Rebischung, and P. Philippsen.** 1997. Heterologous *HIS3* marker and GFP reporter modules for PCR-targeting in *Saccharomyces cerevisiae*. Yeast **13:**1065–1075.